Seamless Multi-Projection Revisited

Petar Pjanic, Simon Willi, Daisuke Iwai, *Member, IEEE*, and Anselm Grundhöfer, *Member, IEEE*

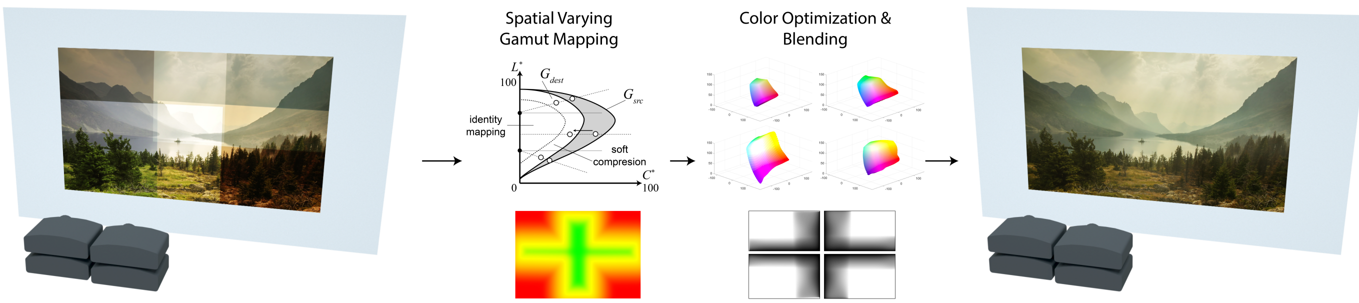

Fig. 1: We propose a novel perceptual-based framework for colorimetrical consistency within a multi-projection display. Using a colorimeter, we establish highly accurate color representations and use them, together with projector overlap information, to generate smoothly spatially varying gamut mappings. We present several approaches to maximize contrast while preserving the target appearance as accurate as possible.

Abstract—This paper introduces a novel photometric compensation technique for inter-projector luminance and chrominance variations. Although it sounds as a classical technical issue, to the best of our knowledge there is no existing solution to alleviate the spatial non-uniformity among strongly heterogeneous projectors at perceptually acceptable quality. Primary goal of our method is increasing the perceived seamlessness of the projection system by automatically generating an improved and consistent visual quality. It builds upon the existing research of multi-projection systems, but instead of working with perceptually non-uniform color spaces such as CIEXYZ, the overall computation is carried out using the RLab [10, pp. 243-254] color appearance model which models the color processing in an adaptive, perceptual manner. Besides, we propose an adaptive color gamut acquisition, spatially varying gamut mapping, and optimization framework for edge blending. The paper describes the overall workflow and detailed algorithm of each component, followed by an evaluation validating the proposed method. The experimental results both qualitatively and quantitatively show the proposed method significant improved the visual quality of projected results of a multi-projection display with projectors with severely heterogeneous color processing.

Index Terms—Projector-camera systems, colorimetric calibration, 3D stereoscopic and multi-user entertainment

1 Introduction

Recent projection mapping attractions use a multitude of projectors to immerse guests in an unprecedented quality. It is not uncommon to have several dozens of devices being superimposed, geometrically registered, and blended together to form a single, consistent image or video screen. High-resolution display walls for information visualization or advertisement as well as modern projection-based virtual reality (VR) systems also tend towards getting scaled in resolution and size, requiring a huge number of projectors being precisely registered. In all these situations, not only a perfect geometrical alignment, but also an accurate consistent colorimetric calibration and adaptation is required to ensure a perceived seamlessness of the overall projection. Especially, consider that devices with varying peak brightnesses as well as color processing pipelines are used. Such configurations lead to an uneven color distribution, especially since each projector inherently has some slight variations in color rendering, even in a homogeneous setup. This effect is potentially even stronger if different projection image generators, such as liquid crystal displays (LCD), liquid crystal on silicon (LCoS), and digital light processing (DLP) engines are mixed, eventually also with varying light sources such as HID/Xenon light bulbs, LEDs, or lasers. Mixing devices is often times preferable, for example, to limit deployment costs of large installations.

The photometric compensation for inter-projector luminance and chrominance variations was widely researched, and the majority of the works were carried out almost a decade ago [14]. Although it seems that most of the important technical issues have been already solved and the research field is matured, we found that previous technologies unfortunately do not work well in lately increasing multi-projection configurations mentioned above, where devices with significantly different color processing components are mixed. An interesting quality evaluation of different color transformation models is given in [11] which clearly shows that non-linear color transformations are required to achieve the maximum quality. To the best of our knowledge, there is no method so far that can alleviate the color non-uniformity at a perceptually acceptable quality among such heterogeneous projectors.

To solve this emerging technical issue, we propose a novel photometric correction technology. Our method has four major technical contributions upon the existing research of multi-projection systems, by which we can achieve perceptually seamless projection even with heterogeneous devices. First, the overall computation is carried out using an optimization in the RLab color appearance model which considers the overall adaptation luminance and thus models the color processing in an adaptive, perceptual manner, while previous technologies worked in perceptually non-uniform color spaces such as sRGB and CIEXYZ. The RLab color space is considered to be a good compromise between the simpler but significantly less accurate CIELAB [10, pp. 199-210] color space and CIECAM02 [10, pp. 287-301] model which is more advanced but much more computationally complex. Second, we propose

- *Petar Pjanic, Simon Willi, Anselm Grundhöfer are with Disney Resaerch. E-mail: {petar, simon, anselm}@disneyresearch.com.*
- *Daisuke Iwai is with Osaka University. E-mail: daisuke.iwai@sys.es.osaka-u.ac.jp.*

Manuscript received 31 March 2007; accepted 1 August 2007; posted online 2 November 2007.
For information on obtaining reprints of this article, please send e-mail to: tvcg@computer.org.

an adaptive color gamut acquisition to accurately estimate the range of displayable colors per device by considering a projector's internal color processing that contains non-linearities as well as potential white boosting or other inter-color modulations (e.g., DLP projectors). The adaptive sampling method automatically decides the sampling points in the RGB color cube to generate an optimized tradeoff between accuracy and acquisition time. Third, considering that overlapping areas are in many cases located around the center of a multi-projection display or at other locations where people frequently look, we propose a spatially varying gamut mapping that utilizes the areas to provide smooth gamut extensions generating color saturations and/or luminance boostings outside of what a single projector can generate. Finally, while previous technologies conduct the color adaptation and edge blending separately, we combine these two processes into an optimization framework in which the alpha values of the blending maps are utilized as a guide to estimate the optimal color contribution for each overlapping device. The method can be scaled to an infinite number of projectors. For speedup and media server integration, the processing can be split up into 3D lookup tables (LUTs) and blending map weights which is a data format currently directly supported by some media server and projectors. This simplifies integration and reduces costs. We conduct an evaluation using a setup consisting of strongly heterogeneous projectors to validate the effectiveness of the proposed method.

In summary, our main contributions are:

- An efficient and adaptive color gamut acquisition to generate an accurate color prediction model
- Operating in the perceptual uniform RLab color space
- A spatially varying color gamut mapping operation generating smoothly varying optimized input target images
- A novel color uniformity optimization method enabling a high-quality projector blending even when using complex non-linear color processing engines

2 Related Work

A typical workflow for accommodating the inter-projector variations is luminance and chrominance matching followed by edge blending [14]. This section introduces prior technologies on these issues and discusses our contributions.

2.1 Luminance and Chrominance Matching

Luminance matching reduces the spacial variation of luminance range across all the projectors of a multi-projection display to achieve brightness seamlessness. A common method finds a conservative luminance range that can be achieved over the whole projection area, and maps the luminance of each projected pixel within the range by multiplying spatially varying attenuation factors [16, 17]. While this is simple and easy to be implemented, it restricts the overall contrast and peak luminance of the multi-projection display to the most limited ones. To enhance the contrast, researchers proposed a spatially varying luminance range guided by the human contrast sensitivity function [13, 18]. The luminance matching approach works well only when color gamuts are the same or similar across the projectors. However, in general, the color gamuts significantly vary among projectors of different models. Consequently, color blotches are visible when a multi-projection display consists of heterogeneous device configuration.

Chrominance matching alleviates the color non-uniformity across projectors. A simple solution is to match the color gamut of each device to a common, conservative gamut that is displayable by all the projectors [15, 31, 36]. This yields a limited dynamic range and color gamut. A more sophisticated method spatially morphs the color gamuts of two adjacent projectors over the overlap region to retain as much of the display color gamut and dynamic range as possible [26]. Because these prior works assume additive color transformations (i.e., color channel independence), the color gamuts of display devices are estimated by measuring the response curve of each channel separately, and consequently, the devices are easily linearized. However, such ideal additive gamuts were not guaranteed when a multi-projection display consists of digital light processing (DLP) projectors which use more than three color components on the output side (RGB plus white or CMY, for example) to boost the brightness and to provide more saturated colors. The non-linearities cannot be just represented by RGB response curves to adjust the input image before processing. A typical solution to deal with non-additive devices is to sub-sample the individual color cubes and interpolate the measurements either linearly [33] or non-linearly [27] to acquire all transformations to the 3D color gamut. The previous works sampled a color cube uniformly (e.g., total of k^3 measurements by k samples per channel). There is a trade-off regarding the determination of k (i.e., large k provides better image quality while leading a unfeasibly long measurement time), which was determined manually in the previous works [27, 33]. Furthermore, to the best of our knowledge, all of the previous technologies worked in perceptually non-uniform color spaces (e.g., sRGB and CIEXYZ).

In this paper, we apply a chrominance matching approach rather than luminance matching to deal with a multi-projection display consisting of devices even with significantly different color gamuts each other. Our approach is not limited to devices which can be linearized easily, but can also work with projectors having non-additive color transformations. We propose an adaptive sampling of individual 3D color cubes, which automatically determines sampling points such that the color transformations to the whole color gamut are accurately acquired after a non-linear interpolation is applied to the sampled measurements. It offers an requirements-specific and optimal trade-off between desired accuracy and measurement time, and also guarantees that the errors are below a desired threshold everywhere in the available color range. Rather than morphing two color gamuts of adjacent projectors, we propose to enhance the luminance and color saturation in the overlapping region, assuming that it locates at the central part of the display and consequently is relatively salient. By this, we provide users with multiple options of color gamuts (i.e., conservative and spatially varying ones) for different application scenarios. Working in a device independent color space which considers the color appearance of the human visual system significantly improves the perceived quality. Therefore, we propose to use RLab color space, which offers a much more accurate perceptual color appearance modeling than sRGB and CIEXYZ.

In contrast to simpler color appearance models such as the CIELAB or CIELUV color spaces, RLab is able to better predict strongly saturated colors by applying a white stimulus adaptation step which is devoid in the former two mentioned color spaces. It is also able to overcome other, well known problems of the CIELAB color space which is the fact that constant hue lines within this space are actually curved, in particular in the blue-magenta region. This can lead to problems when applying color gamut mapping operations. Furthermore, the RLab color appearance model offers additional parameters to adapt more accurately to the observer's viewing conditions by offering an option to adjust the amount of white stimulus adaptation, as well as to account for different intensities of the surrounding stimulus, e.g., adapting to the amount of ambient illumination.

2.2 Edge Blending

Edge blending smoothly connects adjacent projections in the overlapping region where unnatural seams are prominent due to imperfections of luminance or chrominance matching and geometric registration [12, 22–25, 35, 37]. A weight (i.e., attenuation factor) is multiplied with an input color to divide it among overlapping projectors. A widely-adopted method determines spatially varying 2D weight map (blending map) based on the distance from the edge such that the weight value is 0 on the edge. There is room for improvement in the simple edge blending approach. For example, consider a situation where an assigned color is not accurately displayable by the first overlapping projector due to limited color gamut and dynamic range of the device or artifacts caused by luminance and chrominance matchings, and the second projector has a potential to compensate for it. Because current methods separately compute the projection color for each projector, they cannot use the second projector to compensate the error caused by the first projector.

Light transport-based techniques solve this issue by optimizing projection colors such that the difference between a target image and

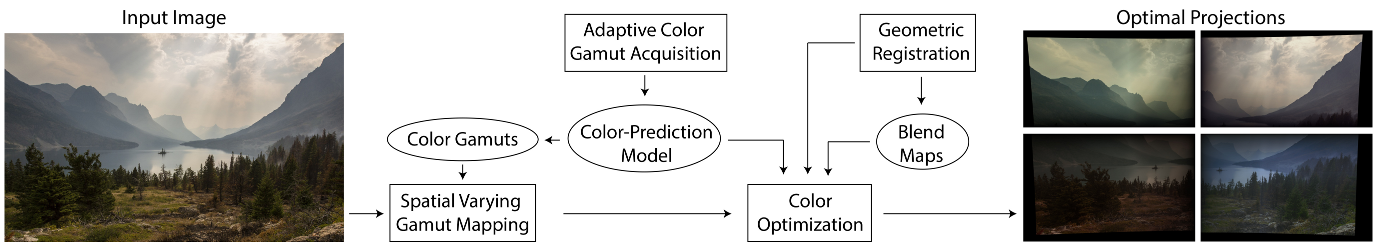

Fig. 2: The core steps of the used color reproduction workflow: Acquiring highly accurate geometric and colorimetric information about the system allows to apply smooth spatially varying gamut mappings. The color optimization incorporating the overlapping information encoded in the blending weight maps to ensure a high-quality result.

estimated projection result is minimized [1–3, 7, 29, 34]. However, these previous methods apply sRGB or CIEXYZ color space and only consider additive color transformations, because the computation of the estimated projection result are represented as matrix multiplications of a light transport matrix with a projection image. Furthermore, assuming the projectors of the same model are used, most of these methods do not explicitly apply any luminance and chrominance matchings.

In this paper, we propose a novel optimization framework that works in RLab color space and deals with non-additive color transformations to achieve perceptually smooth transition in overlapping regions even when different types of projectors including DLP are connected. More specifically, our proposed method uses blending map weights just to guide the amount of different projector contributions to find the optimal color which will, when summed up with all the other projector contributions at each individual pixel, leads to the desired one. All the existing methods using the blending maps directly assign blend values between the different projectors. On the other hand, using the blending maps only as a guidance for amount of color contribution of each individual projector at a given point, but optimizing the colors independent of the blending maps makes the method independent of any unknowns with respect to the non-linear per-color and color mixing behavior of the projectors.

3 Overview

This section overviews the main color reproduction workflow and prerequisite processes.

3.1 Color Reproduction Workflow

We give a high-level overview of the standard color reproduction workflow commonly used in the color community and how it is applied to generate a consistent multi-projection display. It consists of three main components: Estimation of a color prediction model (CPM), gamut mapping, and projection color optimization. Figure 2 illustrates the color reproduction workflow. First the RGB colors of the input image are gamut mapped to a device independent color space. The mapping can either be uniform per projector or spatially varying to account for keystoning, vignetting, and similar effects. These mapped colors represent the target colors that can be reproduced without significant artifacts by the multi-projector system. This gamut mapping operation is guided by a CPM which is used to estimate the volume and shape of the achievable color gamuts. The optimization function relying on the derived CPM is used to deduce what each projector needs to project in order to perceive the colors that are as close as possible to the desired mapped target colors.

Our method is divided into several components. Most of them need to be carried out only once during an initial calibration step: A high quality, but also efficient and adaptive per-projector color gamut acquisition, as well as the target color gamut definition only need to be carried out once. During content generation, gamut mapping and projector color generation has to be carried out. The latter either consists of a simple lookup operation or, if maximum image quality should be the goal and processing time is not a significant limitation, a constrained non-linear optimization process for generating an optimal color reproduction is applied.

We will discuss each of the individual components of this workflow in detail, starting with the adaptive color gamut acquisition required to estimate the CPM (Section 4), gamut mapping (Section 5), and the color optimization strategies for projection image generation (Section 6).

3.2 Prerequisites

To generate a colorimetrically consistent and seamless multi-projection display, several pre-processing steps need to be carried out for system calibration. Since these steps are standard operations, we will only shortly summarize them in the following.

The orientations of the overlapping projectors which should generate a consistent image with respect to the projection surface are usually estimated using a camera. This estimation is carried out, e.g. by projecting predefined patterns, so-called structured light, capturing them and extracting camera-to-projector pixel correspondences. These correspondences then allow to warp an input image such that it is consistently distributed and displayed by all devices.

After geometric registration, projector overlaps can be computed and stored as 2D data structures, defining for each projector pixel, which pixels from all other projectors are illuminating the same surface point. With this knowledge, per-pixel blending weights maps can be calculated to smoothly fade out the contributions from one projector the further it moves into an area of overlapping projections. The result is stored as 2D α-maps defining a color multiplier (within the range of 0.0-1.0) for each pixel. Usually, a distance transform is applied to estimate this factor [24]. To further smooth this maps we applied an additional non-linear diffusion step using successive over-relaxation (SOR) [30]. This approach is similar to the one proposed by Gelb et al. [12] using multiplicative distances, but can be applied in arbitrarily complex geometry in which their method fails.

4 Adaptive Color Gamut Acquisition

To accurately estimate the range of displayable colors per device, their color spaces have to be accurately and comprehensively measured. Especially if the projector's internal color processing is by far not linear but contains non-linearities as well as potential white boosting or other inter-color modulations, it is necessary to not only sample the extremes and the color channels independently, but instead to analyze the full RGB color cube. It is, of course, prohibitive to measure each possible color and thus an efficient sub-sampling scheme needs to be established to precisely acquire the whole color range within a reasonable time frame. We assume that no information about the internal color processing is given and thus propose an adaptive sampling method to generate an optimized tradeoff between accuracy and acquisition time.

4.1 Principle

We measure the reflected colors in the device-independent CIEXYZ color space. In our case sensed by using a colorimeter. This measurement process can be described as:

$$R = E_a + \sum_{i=1}^{n} \delta(i) \cdot E_{rgb}(i) \cdot r \tag{1}$$

where $\delta(i)$ is the binary function defining whether the i-th projector is illuminating the surface at the measurement location, R are the measured values, r is the surface reflectance, $E_{rgb}(i)$ the projected input color of projector i in its native RGB color values and E_a the amount of uncontrollable environmental illumination. All values except $E_{rgb}(i)$ are represented in CIEXYZ additive device-independent colorspace. The values for R are measured independently for each projector i.

To ensure that the overall RGB color cube, i.e. the whole range of colors the projector can reproduce, is sampled sufficiently accurate, we apply a recursive refinement scheme which further samples the cube until all measurements can be reconstructed within a desired accuracy. We use the ΔE^*_{00} [10, p. 83] error metric in CIE Lab color space to assess the accuracy.

The adaptive measurement is carried out using a combination of octree-based and random sampling. In the first step, the eight extreme values of the color cube are sampled. Since we can assume that the behavior inside is most likely non-linear, we also sample additional 19 values to have all RGB colors sampled threefold (all 3^3 permutations of 0%, 50%, and 100% per channel). To further introduce unbiased measurements, we add 16 random samples using Poisson disk sampling [5] and add 16 additional samples in the darkest 10% areas. Having carried out these measurements, we generate the first CPM based on a polyharmonic spline [8], generating a smoothly interpolating and extrapolating mapping which passes through all the measured samples:

$$R(i) = f\left(E_{rgb}(i)\right) \tag{2}$$

This non-linear scattered data mapping was realized using the thin-plate-spline (TPS) function defined as follows:

$$\begin{aligned} f(E_{rgb}) = \sum_{i=0}^{N-1} \omega_i^* \varphi(\|E_{rgb} - q_i^*\|) + \omega_N^* + \\ \omega_{N+1}^* E_r + \omega_{N+2}^* E_g + \omega_{N+3}^* E_b \end{aligned} \tag{3}$$

where $[q_0^* ... q_{N-1}^*] \in Q^*$ are the set of all N projected RGB input samples captured so far and ω_i^* are the $N+4$ TPS weighting coefficients per input color channel, $\|\cdot\|$ the distance in Euclidean space, and φ is chosen to be the TPS radial basis function (RBF):

$$\varphi(d) = \begin{cases} 0, & d = 0 \\ d^2 \log d, & otherwise \end{cases} \tag{4}$$

Details about how to compute the weights ω_i^* of the TPS mapping function can be found in [8].

From that point on, an adaptive refinement is carried out by subdividing the color cube recursively by iterating through it in an octree-based breadth-first manner and (after initializing it by setting each node to "not ready" state) repeating the following steps:

1. If parent node is flagged as "ready", go to (5), otherwise sample, i.e. capture, the RGB value of the center of the current octree entry.
2. Compute an interpolated CIEXYZ result with the RGB value used for sampling in (1) by applying equation 3.
3. Compare the resulting value from (2) to the one measured in (1). The comparison is calculated using the ΔE_{00} error metric.
4. If the difference is below a given threshold t, usually around 1.5-2, the according octree node is flagged as "ready".
5. Proceed to the next node and go back to (1).

We iterate through the octree in a breadth first manner until the interpolation error of all samples is below t, i.e. all nodes are flagged as "ready". Alternatively a predefined maximum number of samples can be set as a stopping criterion if time is a critical factor. Having finished the sampling for an individual projector, we store its whitepoint W^p_{xyz} as well as the measured RGB-to-CIEXYZ correspondence samples. Furthermore, the environmental illumination is measured once as well by turning off all projectors. In the following these values are used to estimate the CPM used to define the available color gamuts and to carry out the optimal color transformations needed for generating a high-quality seamless multi-projection display.

4.2 Accounting for Intra-Projector Variations

Since a colorimeter is used as measurement device, the sampling is carried out in device independent colors which ensures highly accurate results. However, the sampling is limited to a specific small region and thus the potentially significant *intra-projector* variations [6] are not considered. To account for them efficiently, we propose to additionally sample different projection areas, but only for it's peak luminance by projecting white. This measured sample then is used to remap the whole color cube of the full measurement which has been carried out in the projection center. This is reasonable since the spatial variations mainly occur in the luminance values, but are almost negligible with respect to its chromimance since they are mainly caused by lens vignetting and other imperfections of the optical path, but the projector's color processing is spatially uniform. Having sampled the spatially varying peak luminance, a smooth per-pixel adjustment map is generated to determine a per-pixel color gamut by interpolating between the measured ones.

5 Color Gamut Mapping

Having sampled each projectors' input RGB color cube as well as the environmental illumination provides us with all the information needed to compute an accurate CPM. With this, the maximum available color gamuts for generating a perceptually uniform and consistent color reproduction can be estimated. In this step, the input RGB values of the images to display are mapped to a device independent working color space. We chose to use the RLab color space [9] [10, pp. 243-254] which is an extension of the CIELAB space that enables more accurate color appearance predictions since it considers chromatic adaptation, the displaying media, as well as relative luminance and surround stimulus adaptation.

Having transformed the input colors into this target space, they need to be mapped into a range which can be accurately reproduced by the projectors. This mapping depends on various factors, such as the user's intent, i.e. the desired visual effect that should be achieved, but also several other factors influence the gamut mapping strategy, such as the input RGB values, which and how many projectors are projecting it, whether a spatially varying or a uniform gamut mapping is desired and if intra-projector variations should be considered (cf. Sec.4.2). We will discuss gamut mapping strategies considering these factors in the following.

5.1 Estimation of the Available Color Gamuts

Since the mapping is carried out in RLab space, an overall approximation of the color gamut needs to be defined for each projector within this space. Obviously, each device defines its own, unique, gamut, i.e., the volume describing all the colors that the projector can reproduce. In the simplest case, we ignore any intra-projector variations and define one gamut per projector by using the data acquired as described in section 4.

For the overall multiprojection system, we define one unique CIEXYZ color as target white point. This is manually chosen depending on the user's intend, for example, by measuring the reflected white of the projector which appears to be neutral when projecting full RGB white. Using the mapping function as defined in Equation 2, we predict the CIEXYZ values for a regularly spaced set of samples of the RGB color cube and convert those predicted values into their RLab color representation. Finally, after having transformed all colors into the RLab space, their concave hull is computed, e.g. by using the method described by Moreira et al. [19] to define the color gamut for each individual projector by a 3D polygon.

Next, the combined gamuts of different projectors are estimated: If an area is illuminated by more than one device, brighter colors can be generated than using only a single projector. However, also the black level is added in this area which again reduces the achievable contrast. These gamuts are computed for all combinations of different

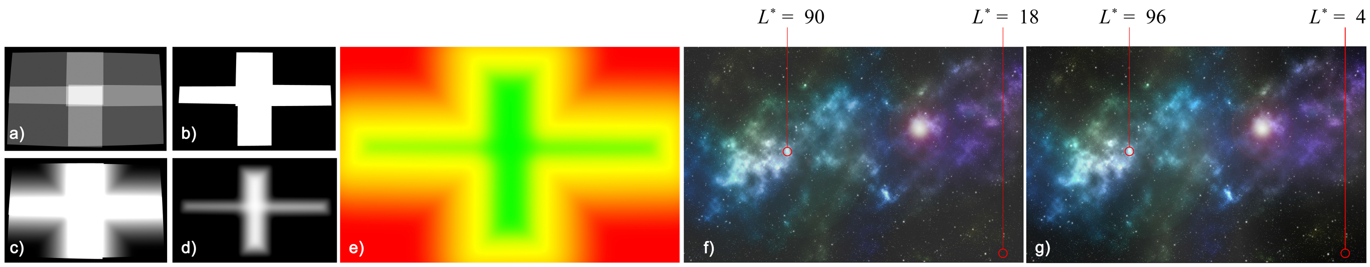

Fig. 3: Illustration of the spatially varying gamut mapping in a four-projector setup. The overlapping regions are detected and smooth gamut transition maps are generated. They are used to maximize contrast by spatially mapping the input colors to different dedicated color gamuts. Figure (a) shows the proposed four-projector setup, (b) is the region where projectors are overlapping, (c) and (d) are distance transform functions used to establish smooth mapping between different gamuts and (e) is the final gradient map guiding the gamut mapping process. In (e) the red color represents mapping to the individual projector gamuts, yellow represents mapping to the gamut defined for the edge of the overlapping area and green represents mapping to the gamut defined for inside of the overlapping area. A comparison is shown in the sample result images on the right hand side: (f) shows a uniform, convervative mapping, while in (g) the spatially varying approach is applied. The two selected L* values show the luminance differences which are achieved in this example using this method.

overlaps. These areas are automatically computed during the geometrical calibration described in Section 3.2. For each overlapping projector combinations, we apply Equation 1 for a sub-sampled set of RGB input values, using the individual CPMs estimated as described in Section 4. The resulting XYZ values are converted into the RLab color space using the same white point as before and again the concave hull is computed. In addition to these gamuts, we also compute the overall common gamut which defines the conservative range of colors which can be reproduced by all devices. Therefore the intersection volume of all previously calculated gamuts (including both projector gamuts and multi-projector gamuts) is computed.

At this point we have an exact definition of the colors which can be reproduced for any position on the illuminated surface. If intra-projector variations should be considered as well, this definition changes for each pixel area. As stated beforehand, this can be computed by measuring the gamut at multiple locations per projector and interpolating between the measurements.

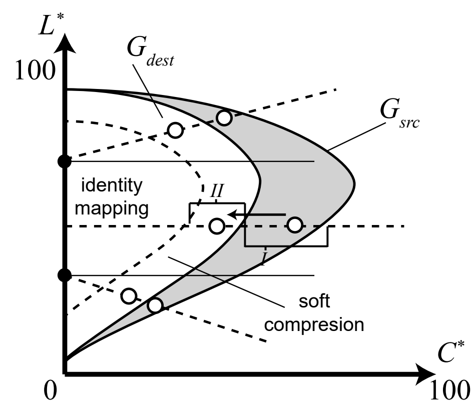

Fig. 4: Schematic visualization of the chroma mapping step during the gamut mapping operation for a lightness adapted source G_{src} and target gamut G_{dest} in RLab space (Please refer to Sec.5.2 for details).

5.2 Input Color Gamut Mapping

With the knowledge about the displayable range of colors, we can now map any input image to the displayable target gamut. Therefore, the input images' native color representation, usually defined as sRGB, Adobe RGB, etc., is transformed to the target output gamut which reproduces the desired input colors as close as possible. The applied gamut mapping operation is defined as follows. First, the input colors are converted to RLab color space in which the gamut mapping method described by Morovic and Luo [21] is applied. It divides the operation into three parts: (1) gamut preprocessing, (2) lightness mapping and (3) chroma mapping. During gamut preprocessing input gamut is adjusted to better fit to the target. Therefore, the white points and hues could be adjusted to better match each other [20, pp. 203-205]. Since this can have a significant impact on the image appearance, it has to be applied carefully.

After the white point alignment, the input lightness is mapped to the range (L^*) of the target gamut in a linear manner. Finally, during the chroma mapping, the actual gamut mapping operation is carried out ensuring that the input colors are all mapped into the range of the target gamut. Figure 4 visualizes this process. First, the white and black points of the target gamut are defined. Then, two focal points are specified on the axis between them. They divide the space into three parts. In the area between both focal points, the chroma is mapped along the lines of constant lightness, i.e., lines which are parallel to the C^* axis. Outside of this range, –chroma is mapped along lines starting from the focal point going to the value to map. More details about this operation can be found in [21] [20, pp. 203-240].

5.3 Spatially Varying Gamut Mapping

As stated in Section 5.1, several gamuts can be defined, depending on whether a single or multiple projectors illuminate the surface area. Since on the one hand the overall contrast and brightness of the projection should be maximized while on the other hand the overall image should appear spatially close to uniform or at least consistent without clipping artifacts, different mappings can be carried out. The simplest solution would be to not apply any gamut mapping, accepting potential clipping artifacts if the color cannot be reproduced (without g.m.). Another approach would be to map the whole content into the conservative gamut which ensures that all input colors can be reproduced by eventually significantly sacrificing peak luminance and overall contrast (conser. g.m.).

Applying a spatially varying color gamut mapping is a solution in balancing a trade-off in image modification and contrast maximization. Obviously, this is a method which has to be carried out carefully to ensure that the image modifications are minimal and smoothly applied to avoid the generation of unwanted image alterations. We propose a method that, by using distance transform, smoothly blends between three different gamut regions: the individual projector gamuts, gamuts being defined for the edges where projectors overlap and gamuts for inside the overlapping areas (sp. var. g.m.). In our setup, for spatially-varying gamut mapping, we used the common-conservative gamut for the edges of the overlapping area and all projectors overlapping color gamut for inside the overlapping area, however user can define other gamuts depending on the desired observable appearance. Figure 3 schematically illustrated the mapping process.

Having carried out that step, the image is ready for being transformed back into the original per-projector RGB representations and can be used as input for the final projection image generation which will be described next.

6 Projection Image Generation

With the acquired data, an accurate target color gamut can be estimated and the input image can be mapped into it, as described previously. This can be either globally fixed or spatially. However, in any case, it has to be estimated what each projector needs to project to generate an as-accurate-as-possible color appearance to the desired one. In the following we will present the overall optimization workflow and discuss several realizations.

6.1 Classical Post-Processed Blending

As summarized in the related work section, most of the previous work applied projector color generation and blending as two separate steps. We implemented this approach as follows. Assuming that the content is already gamut mapped, the projector-individual CPMs are utilized and the projector colors are optimized for the current projector by applying:

$$rgb_i^{opt} = \underset{rgb_i}{\arg\min}(\Delta E_{00}(RLab_{trg}, RLab(rgb_i))) \tag{5}$$

where rgb_i^{opt} is the optimal projection values that should be projected by the i-th projector, ΔE_{00} is the error metric quantifying the difference between two colors in RLab color space, $RLab_{trg}$ is the target color that we want to observe, and $RLab(rgb_i)$ is the colors that can be reproduced by the i-th projector.

The blending weights are then incorporated by estimating the device's response curves of the individual color channels using the measured XYZ values:

$$rgb_i^* = G_i(rgb_i) \tag{6}$$

and its inverse:

$$rgb_i = G_i^{-1}(rgb_i^*) \tag{7}$$

where rgb_i^* is the linearized color values of the i-th projector and G_i is the function describing the response curve of the i-th projector (i.e., a gamma function in the ideal case). G_i^{-1} is the inverse function of G_i.

Using the functions, the corrected, blending-weight adjusted projection images can be generated by:

$$rgb_i^{opt\alpha} = G_i^{-1}(\alpha_i \cdot G_i(rgb_i^{opt})) \tag{8}$$

This approach has its benefits since it is simple to apply it and can also be realized straightforward for real-time and interactive applications by pre-computing the 3D color transformation and storing them as LUTs.

However, it has disadvantages as well since some assumptions are made which might be infeasible in real-world installations: Some projectors, especially low-end DLP devices tend to have strong color and intensity dependent internal color processing which makes it hard to successfully estimate the response curves accurately. Furthermore, black-levels are also not directly considered. To account for the black levels, the blending function (Equation 8) needs to be modified to:

$$rgb_i^{opt\alpha} = L_i^{-1}(\alpha_i \cdot L_i(rgb_i^{opt}) - \sum_j^n \beta_j L_j(bl)) + L_i(bl) \tag{9}$$

Where L_i is a function mapping input RGB values to linearized CIEXYZ Y values, L_i^{-1} is the inverse function, β is equal to 1 if the n-th projector illuminates this point, 0 otherwise. $L_n(bl)$ is the luminance value of the black level of the n-th projector.

However, even when accounting for the black levels, the complex color modulations of the projectors are degrading the overall accuracy as we will show in Section 7. Furthermore, if a subset of overlapping projectors cannot reproduce the target color, the other projector can not be used to compensate for this limitation with this approach since each projector is treated independently.

6.2 Unconstrained Optimization

To overcome the limitations of the classical post-processed blending approach, the optimization method can directly consider the contributions of all projectors by minimizing the color difference between the target gamut mapped color and a color which can be reproduced by the combination of all devices:

$$\begin{aligned} &\left\{rgb_1^{opt}, ..., rgb_n^{opt}\right\} = \\ &\underset{rgb_1,...,rgb_n}{\arg\min} \left(\Delta E_{00}\left(RLab_{trg}, RLab\left(rgb_1, ..., rgb_n\right)\right)\right) \end{aligned} \tag{10}$$

where $\left\{rgb_1^{opt}, ..., rgb_n^{opt}\right\}$ are the optimal RGB projection values that should be projected for all n projectors illuminating the considered region, and $RLab\left(rgb_1, ..., rgb_n\right)$ are the colors that can be reproduced by the illuminating projectors.

With this basic optimization, images with the desired color appearance can be computed and projected. Since this approach requires a per-pixel color optimization of all projector colors it is relatively slow and thus might not be very suitable for animated or interactive content. Furthermore, it can create noisy projections since in areas with multiple overlapping projectors, a single color can be obtained using a multitude of different combinations of superimposed colors. The more projectors are overlapping the more this issue becomes pronounced.

The performance can be increased by pre-processing the mapping operation and storing it in sub-sampled per-projector LUTs, and interpolating between the values. However, even when using LUTs, this approach does not handle the noise issue, and secondly, the final interpolation is carried out in projector RGB space which, due to its non-linearities, might not well suited for interpolation.

6.3 Strategies to Overcome the Unconstrained Optimization Issues

To overcome the issues of the unconstrained optimization while still be able to preserve a high color reproduction accuracy, we propose two novel approaches which can be used to generate high quality results while overcoming the mentioned limitation at the same time.

6.3.1 Constrained Optimization Using Blend Maps

To generate an optimal result which is independent on the accuracy or availability of any response functions, we propose a constrained optimization to generate a noise-free, high quality result. The main idea is to constrain the projectors' RGB space by using the already computed blending weight maps (cf. Section 3.2) as a guide for calculating the smooth transition between all projectors. After having carried out the gamut mapping as described in Section 5, for each projector $(i = 1, ..., n)$ at every pixel location (x, y), Equation 10 is computed to determine the optimal projection colors, but with a constraint on the RGB values as follows:

$$\frac{rgb_1^{opt}}{\alpha_1} = \frac{rgb_2^{opt}}{\alpha_2} = ... = \frac{rgb_n^{opt}}{\alpha_n} \tag{11}$$

where $\alpha_1, ..., \alpha_n$ are the alpha values stored in the blending maps for the according pixel location (x, y). This constraint states that all projectors should project similar hue values but at different intensity value. I.e. if α_i is small and close to 0, the according values of rgb_i^{opt} should also be small and will have only a small contribution to the observed color. In contrast, when α_i is close to 1, the according rgb_i^{opt} has a strong influence to the observed color. The important factor, however, is the fact that this approach constrains the output color to a compromise which is only able to smoothly change depending on the blending map values and thus successfully suppresses noise. Without this constraint, neighboring pixel intensities in overlapping areas might be composed out of strongly varying color contributions per projector which would immediately lead to color artifacts in the case of even slight misalignments which should obviously be avoided. Another option to ensure smoothness would be to apply a global optimization approach considering the local neighborhood using smoothness terms. This, however, would required a more complex optimization strategy and much more computational overhead, so we decided to focus on a constrained local optimization.

However, when a large number of projectors are used, this constraint optimization might start to converge slowly due to its growing dimensionality and the strong constraint between the inputs. To overcome this issue, we can incorporate the constraint directly into the function to minimize:

$$rgb_{\text{int}}^{opt} = \underset{rgb_{int}}{\arg\min}(\Delta E_{00}(RLab_{trg}, RLab(\alpha_1 \cdot rgb_{int}, ..., \alpha_n \cdot rgb_{int}))) \tag{12}$$

where

$$rgb_1^{opt} = \alpha_1 \cdot rgb_{int}^{opt}, \ldots, rgb_n^{opt} = \alpha_n \cdot rgb_{int}^{opt} \tag{13}$$

$$rgb_{\text{int}}^{opt} \in [0, \frac{1}{\max(\alpha_1, ..., \alpha_n)}] \tag{14}$$

With this approach an intermediate projection value rgb_{int}^{opt} is introduced to calculate the final n output values $rgb_1^{opt}, ..., rgb_n^{opt}$. Instead of optimizing for n different projection values that fit a given constraint, now only one constrained intermediate projection value needs to be estimated.

Even with this approach the fact that the optimization function needs to be applied for each pixel position (x, y) slows down the projection image generation. To overcome this problem, one might pre-calculate the results for all possible combinations of $RLab_{trg}$ and $\alpha_1, ..., \alpha_n$ values. However, depending on how densely this space needs to be sampled, the table might become too large since the dimension scales with the number of projectors used.

6.3.2 Pre-Processed Blending

If real-time performance or interactivity is required, the constrained optimization approach becomes infeasible. To enable fast processing while still keeping the image quality at a high level, another approach can be carried out which, instead of considering all projectors at every location, treats each projector independently by pre-computing an optimized color processing pipeline. By combining this processing with an image adaptation using the blending map weights to distribute the color contribution the projector should reproduce, results with similar image quality compared to the optimization approach can be achieved.

Again it is assumed that the input projection image colors are already gamut mapped. These $RLab_{trg}$ values are then transformed back into CIEXYZ color space (XYZ_{trg}) and the blending map weights are used to separate this color into n individual components $XYZ_{trg}^1, ..., XYZ_{trg}^n$, one for each projector:

$$XYZ_{trg}^i = \alpha_i \cdot XYZ_{trg} \tag{15}$$

Since the α values are all constrained to sum up to one at each spatial position, we can define:

$$XYZ_{trg} = \sum_i XYZ_{trg}^i \tag{16}$$

However, since each projector is containing a small amount of uncontrollable light contribution, this definition has to be extended to:

$$XYZ_{trg}^i = \alpha_i \cdot (XYZ_{trg} - \sum_j^n \beta^j XYZ_{blck}^j) + XYZ_{blck}^i \tag{17}$$

where XYZ_{blck}^n is the CIEXYZ value of the black level for the n-th projector and β^n is 1 if the n-th projector illuminates this surface point and 0 if not.

If each of the projectors are able to reproduce its own target color XYZ_{trg}^i the desired target color XYZ_{trg} will be generated. This enables a separation of the optimization function and can be carried out independently for each projector:

$$rgb_i^{opt} = \underset{rgb_i}{\arg\min}(\Delta E_{00}(RLab_{trg}(XYZ_{trg}^i), RLab(rgb_i))) \tag{18}$$

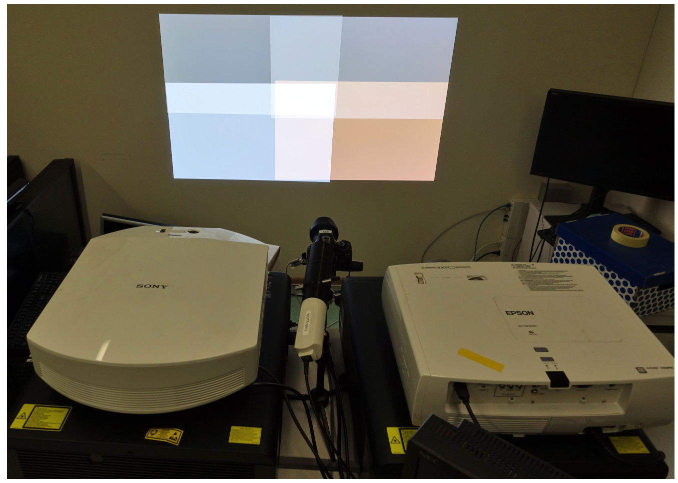

Fig. 5: The experimental four projector setup. As it can be seen, the projected uncalibrated white significantly differs between all devices.

This optimization function computes the RGB values to project to obtain the XYZ_{trg}^i. Since this is independent for each projector, the results can be precomputed and stored as a 3D LUT to directly lookup the projection colors. Besides fast computation, this approach has the benefit that the pre-processed blending weights allow to still account for any complex response curve processing such as white boosting for any color correction that projector may apply. However, compared to the overall optimization approach discussed in Section 6.3.1, this approach is not able to let one projector compensate for out of gamut errors of another projector in overlapping areas.

6.4 Summary

We proposed two novel projection image generation methods which slightly vary in the overall image quality, but are superior to straightforward post-processed blending operations in which the color adaptation and blending are treated as separate operations, since, practically, the color processing of most projectors makes the response curves vary per channel or even depending on the input color values. The problem of generating simple, single channel response curves to linearize input images is resolved by incorporating the blending weights directly into the computation of the final projection color. In the following we will present our experimental setup, evaluate and compare results and discuss them.

7 Evaluation and Discussion

We evaluated the proposed method using a heterogeneous multi-projector configuration consisting out of four overlapping projectors. This was chosen as the main evaluation platform since its heterogeneous devices presents a worst-case solution for a multi-projector display but it still is simple to allow us to focus closely on the actual image quality. Two of them were professional, single-channel DLP projectors[1]. They have been configured to generate significantly different outputs, in terms of color, luminance as well as response curves. In addition, a LCoS projector[2] was used as well as a three-chip LCD device[3]. They all were deliberately manipulated to show significantly different color characteristics as illustrated in Figure 5, showing a full white projection[4].

In the first step, the geometric calibration was carried out using binary structured light blob patterns and a DSLR for acquisition [5]. The

[1] 2x Panasonic PT-RZ770

[2] Sony VPL-HW40ES

[3] Epson EH-TW3200

[4] Please note that this has been carried out to make the performance of our proposed method more visible in the figures

[5] Canon EOS 1200D, Samyang 14mm f/2.8 lens

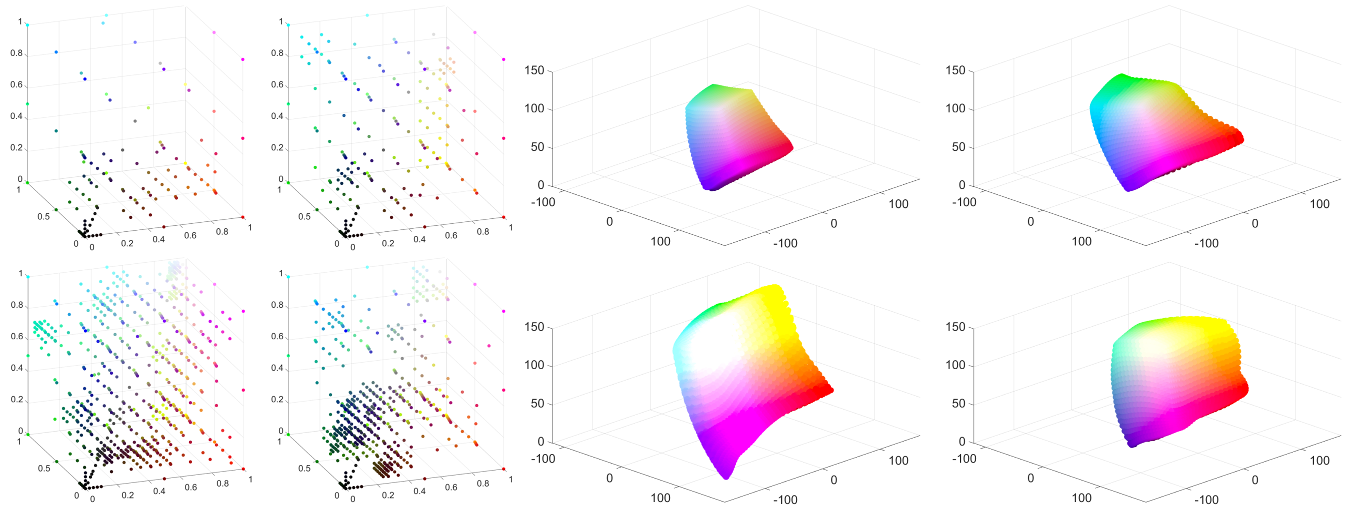

Fig. 6: Left: The adaptively computed RGB input samples. As it can be seen the sampling refined the RGB cube significantly different depending on the device. Right: The according interpolated color gamuts in RLab space for all four projectors. They are ordered as they are located physically (cf. the configuration shown in Figure 5): The two lower ones are the Panasonic DLPs, the upper left the Sony LCoS and the upper right the Epson LCD device.

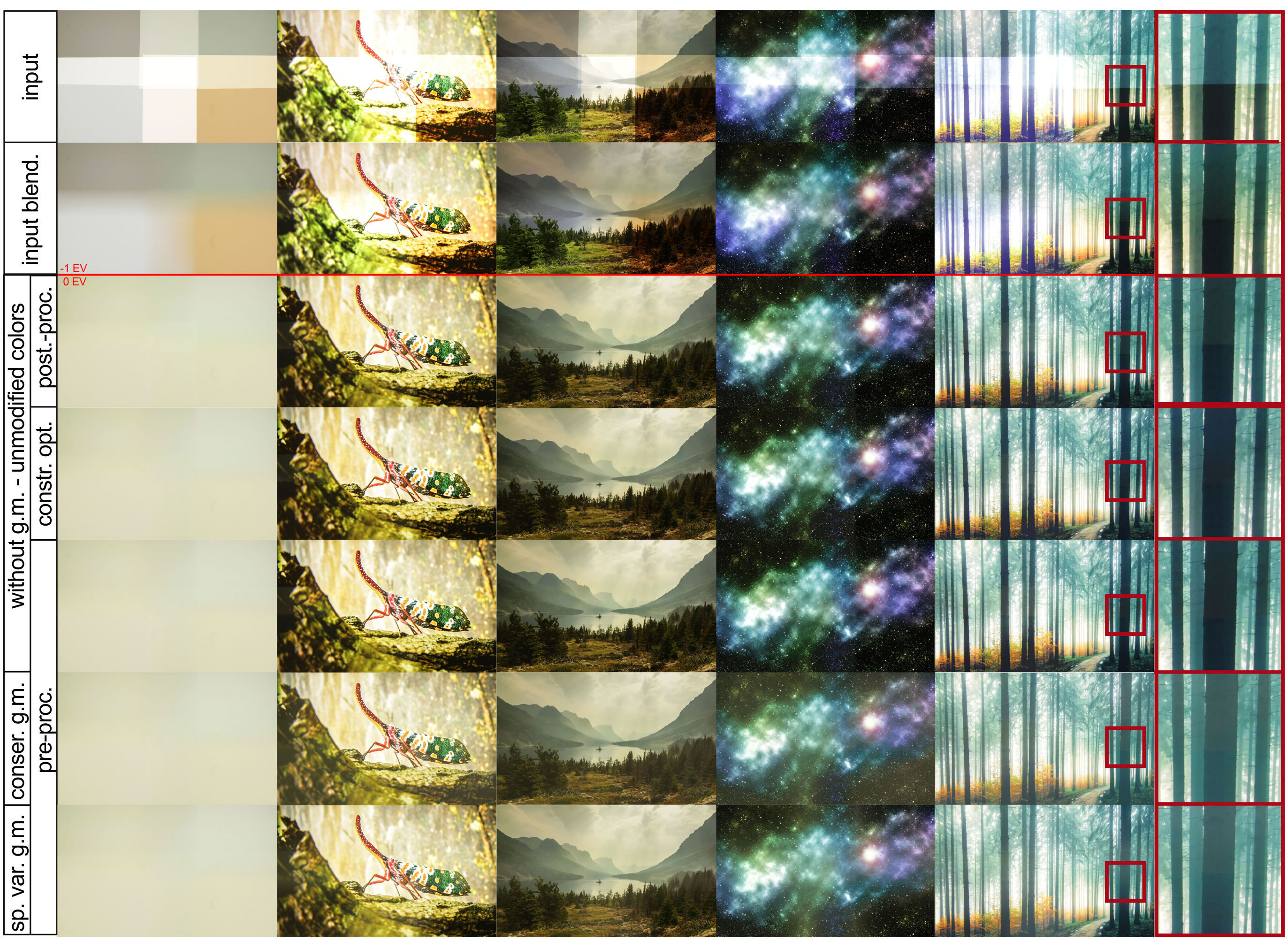

Fig. 7: Comparison of several projected images: The top two rows are showing the input images without any gamut mapping or color optimization applied. (They were captured with half the exposure time to avoid saturation). The bottom five rows show the different gamut mapping and optimization approaches.

resulting warping tables were used to transform all evaluation images into the according perspectives of the projectors. Blending weight maps were computed as described in Section 3.2. Next, the individual color gamuts were acquired with a colorimeter[6] using the adaptive sampling strategy which has been summarized in Section 4. A ΔE_{00} threshold of 1.5 was used. The RGB inputs and the resulting measured samples of all four projectors are visualized in Figure 6[7]. As it can be seen, the adaptive sampling algorithm had to carry out significantly different strategies to achieve a mapping accuracy below the given target threshold. Depending on the device, 111 up to 664 samples were required to achieve the desired CPM accuracy. Each of the samples was captured 15 times and averaged to minimize temporal variations due to the potential temporal effects of the color processing engines used such as mirror flips or dithering [4]. The overall scanning took approximately 30 minutes.

The code was implemented prototypically in Matlab and ported to C++. The constrained optimization described in Section 6.3.1 was implemented using a box constrained non-linear solver with numerical differentiation[8]. Note that discontinuities in the CIE2000 function [28] makes it impractical to use analytical gradients. By utilizing exhaustive parallelization and caching, the per pixel constrained optimization approach for a set of four projection images for the proposed setup shown in Figure 5 could be calculated in approx 5-10 minutes[9]. Results as well as comparisons to the other proposed approaches will be shown in the following.

7.1 Results

Figure 7 shows a comparison of the proposed methods for several images using the four projector setup. We compared seven conditions where different gamut mapping and color optimization methods were applied. The first two were baseline conditions where no gamut mapping or color optimization was applied. In the first condition (input), only the geometric registration using structured light pattern projection method described in Sec. 3.2 was applied. In the second baseline condition (input blend.), a simple blending method also described in Sec. 3.2 was additionally applied. The other five conditions were prepared by combining different gamut mapping and optimization approaches. For gamut mapping, we show the methods of without gamut mapping (without g.m.), conservative gamut mapping (conser. g.m.) and spatially varying gamut mapping (sp. var. g.m.), which are described in Sec. 5.3. For color optimization approach, we show the methods of post-processed blending (post-proc.) in Sec. 6.1, constrained optimization (constr. opt.) in Sec. 6.3.1, and pre-processed-blending (pre-proc.) in Sec. 6.3.2.

Comparing the baselines (top two rows in the figure) and the others, we find that significant improvements in image quality are achieved by gamut mappings and color optimizations. Different gamut mapping and color optimization methods can be compared by focusing a dark region as shown in the right most column. The visibility of the black level edges are more diminished in const. opt. and pre-proc. than post-proc. Therefore, by integrating the alpha values into the optimization process, the overall already good image quality can be further improved, especially when the response curves are color dependent as it is the case in the given configuration of the evaluation setup[10]. From the same focused region, it can be seen that the visibility of the black level edges are more diminished either by conser. g.m. and sp. var. g.m. than without g.m. Therefore, our gamut mapping methods worked well.

7.2 Evaluation

Since the photographs in the figures make it difficult to accurately assess and compare the image quality of the different methods, we objectively

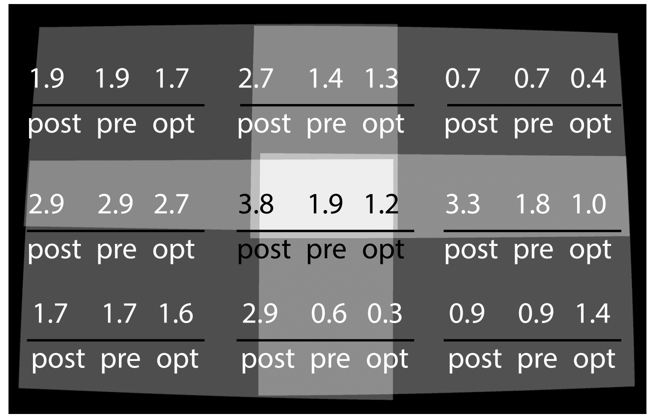

Fig. 8: Color accuracy for each region of a projected uniform white color expressed in ΔE_{00} color differences. The figure shows a photograph of the unblended projections to highlight the projector overlaps.

Table 1: Spatially-average color variations from the target colors expressed in ΔE_{00} color differences.

mean ΔE_{00}	White	Gray	Red	Green	Blue	Black
post-proc.	2.35	2.1	1.5	1.1	1.6	2.52
constr. opt.	1.34	1.33	1.24	0.89	1.1	1.5
pre-proc.	1.58	1.44	1.42	0.99	1.5	1.57

evaluated the quality of our approach by firstly measuring the reflected colors using the colorimeter at different spatial locations and secondly by setting up a second two-projector configuration to evaluate the quality when using spatially varying color prediction models.

7.2.1 Color Uniformity Measurements

Since the camera images are not exactly giving an objective impression of the quality of our method, we carried out further measurements: To evaluate the uniformity which can be achieved with our presented approaches, we displayed several uniform colors being processed by the different color optimization methods. The reflected colors were sampled by the colorimeter at 9 different locations and analyzed.

Figure 8 shows ΔE_{00} values between the measured and the expected input XYZ values for a gamut mapped full white image at the nine sampled locations for the different approaches. As it can be seen, the proposed CPM is able to accurately reproduce the desired colors. Furthermore, it shows that the pre-processed blending as well as the constrained optimization approaches are able to significantly further improve the accuracy compared to a post-processed blending approach. This becomes obvious when comparing the five measurement areas where the different projectors overlap.

In table 1, the averaged ΔE_{00} values for the nine sample locations are listed for six different uniform color projections. Again, it can be shown that our CPM is able to accurately reproduce the target colors. Furthermore, it also shows that the additional computational overhead of using the constrained optimization approach leads to the most accurate color reproduction.

7.2.2 Spatially Varying Color Gamut Mapping

Figure 9 shows two interleaved photographs of a projection generated by gamut mapping the content to a conservative gamut and one using the spatially varying gamut mapping approach. One can observe that by using the latter, we are able to achieve a higher contrast, i.e. darker blacks as well as brighter highlights, without generating any color clipping artifacts.

7.2.3 Spatially Varying Color Prediction Models

As mentioned in section 4.2, our method is also able to account for spatially varying CPM within one projection. This is, for example, required if the projector is illuminating the surface from a steep angle.

[6] Klein K10-A

[7] The consistent target white point was manually chosen to represent neutral white. Because of that, some values exceed 100 on the L axis.

[8] ALGLIB (www.alglib.net), Sergey Bochkanov

[9] Intel Xeon E5 2643-v4, 64 GB RAM

[10] It should be mentioned that the lower two Panasonic DLP projectors had an uncontrollable black frame around the pixel area of the DLPs. This was not considered in our approach

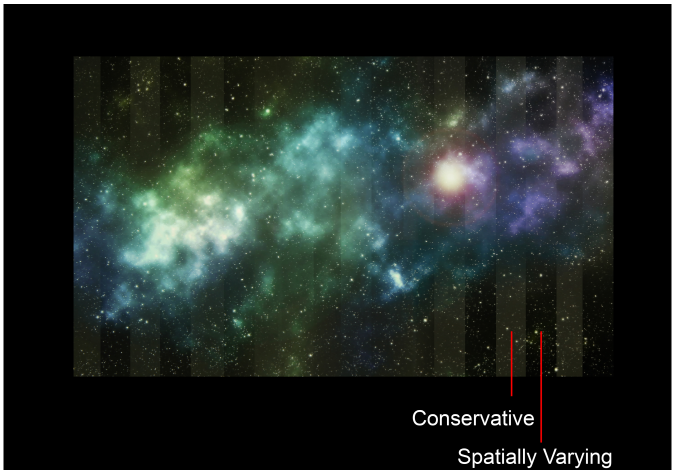

Fig. 9: Interleaved photograph of the projections where even stripes are mapping to a conservative gamut and odd stripes to a spatially varying gamut.

To evaluate how well such intra-projector variations can be handled, we set up a second prototype consisting of two projectors (LCoS and LCD) in a horizontal cross-configuration. The results are shown in Figure 10. In (a), the photograph of an uncorrected grey projection is shown. The numbers show the ΔE_{00} errors for corrections using spatially uniform and varying CPMs. The result of the latter is also shown in the photograph (b) in which a uniform gray projection is generated.

7.3 Limitations

Although the proposed method is able to generate a high quality multi-projection displays even in heterogeneous projector configurations and with devices which are difficult to linearize, it still has limitations: The proposed method does not consider black levels outside the projector pixel area which is an issue for most DLP projectors. Since this area is uncontrollable it can not be directly controlled but the other overlapping projectors could be used to compensate for that offset. However, an accurate knowledge of that area then is required which could be carried out using the camera by thresholding individual black projections. This, is one of the points which we are targeting to investigate in the future.

8 Summary and Conclusions

Our proposed framework for generating a consistent, uniform, high-quality multi-projection display offers flexible but still efficient methods to achieve that goal, even when heterogeneous projectors are used which do not have linear responses and cannot be linearized easily due to their complex color processing operations. The experimental results showed that our pre-processed blending and constrained optimization methods provided superior visual quality to the classical post-processed blending method in terms of luminance and color uniformity. In the future, considering a display system consisting of a large number of projectors, we are planning to apply a distributed cooperative optimization framework (e.g., [32]) to avoid a significant increase in computational costs. Carrying out an in-depth evaluation of the perceived visual quality with accurately tuned RLab parameters regarding varying levels of ambient illumination and color adaptation, as well as implementing and evaluating other, eventually even more sophisticated color appearance spaces is another interesting direction of future research.

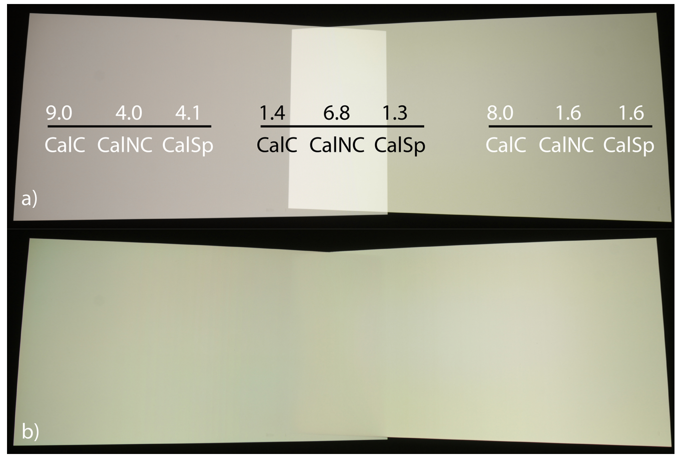

Fig. 10: Results using two projectors in a strongly keystoned configuration. Figure (a) shows the spatial ΔE_{00} difference between the measured color and the target color (RLAB =(57,0,0)) for CalC - model calibrated with one measurement position per projector taken at the center observed image, CalNC - model calibrated with one measurements position per projector taken at left and right of the center image, and CalSp - model calibrated with two measurement position for each projector accounting for the distance light drop of. As one can observe, a model taken with only one spatial measurement is not able to generate a consistent image and accurate blending. Figure (b) shows smooth and spatially consistent projection of the target gray color (RLAB =(57,0,0)) with model calibrated with two different measurement positions.

References

[1] B. Ahmed, J. H. Lee, Y. Y. Lee, and K. H. Lee. Projector primary-based optimization for superimposed projection mappings. *Journal of Electronic Imaging*, 27:27 – 27 – 17, 2018. doi: 10.1117/1.JEI.27.1.011011

[2] D. G. Aliaga, Y. H. Yeung, A. Law, B. Sajadi, and A. Majumder. Fast high-resolution appearance editing using superimposed projections. *ACM Trans. Graph.*, 31(2):13:1–13:13, Apr. 2012. doi: 10.1145/2159516.2159518

[3] A. Bermano, P. Brüschweiler, A. Grundhöfer, D. Iwai, B. Bickel, and M. Gross. Augmenting physical avatars using projector-based illumination. *ACM Trans. Graph.*, 32(6):189:1–189:10, Nov. 2013. doi: 10.1145/2508363.2508416

[4] M. S. Brennesholtz and E. H. Stupp. Projection displays. 2008.

[5] R. Bridson. Fast poisson disk sampling in arbitrary dimensions. In *ACM SIGGRAPH 2007 Sketches*, SIGGRAPH '07. ACM, New York, NY, USA, 2007. doi: 10.1145/1278780.1278807

[6] M. Brown, A. Majumder, and R. Yang. Camera-based calibration techniques for seamless multiprojector displays. *IEEE Transactions on Visualization and Computer Graphics*, 11(2):193–206, Mar. 2005. doi: 10.1109/TVCG.2005.27

[7] N. Damera-Venkata, N. Chang, and J. Dicarlo. A unified paradigm for scalable multi-projector displays. *IEEE Transactions on Visualization and Computer Graphics*, 13(6):1360–1367, Nov. 2007. doi: 10.1109/TVCG.2007.70536

[8] J. Duchon. Splines minimizing rotation-invariant semi-norms in sobolev spaces. In W. Schempp and K. Zeller, eds., *Constructive Theory of Functions of Several Variables*, pp. 85–100. Springer Berlin Heidelberg, Berlin, Heidelberg, 1977.

[9] M. D. Fairchild. Rlab: a color appearance space for color reproduction, 1993. doi: 10.1117/12.149061

[10] M. D. Fairchild. *Color Appearance Models*. The Wiley series on imaging science and technology. Wiley, New York, 2013. A Wiley-Interscience publication.

[11] A. Grundhöfer and D. Iwai. Robust, error-tolerant photometric projector compensation. vol. 24, pp. 5086–5099, 2015.

[12] M. Harville, B. Culbertson, I. Sobel, D. Gelb, A. Fitzhugh, and D. Tanguay. Practical methods for geometric and photometric correction of tiled projector. In *2006 Conference on Computer Vision and Pattern Recognition Workshop (CVPRW'06)*, pp. 5–5, June 2006. doi: 10.1109/CVPRW.2006.161

[13] A. Majumder. Contrast enhancement of multi-displays using human contrast sensitivity. In *2005 IEEE Computer Society Conference on Computer Vision and Pattern Recognition (CVPR'05)*, vol. 2, pp. 377–382 vol. 2, June 2005. doi: 10.1109/CVPR.2005.111

[14] A. Majumder and M. S. Brown. *Practical Multi-projector Display Design*. A. K. Peters, Ltd., Natick, MA, USA, 2007.

[15] A. Majumder, Z. He, H. Towles, and G. Welch. Achieving color uniformity across multi-projector displays. In *Proceedings Visualization 2000. VIS 2000 (Cat. No.00CH37145)*, pp. 117–124, Oct 2000. doi: 10.

1109/VISUAL.2000.885684

[16] A. Majumder and R. Stevens. Lam: Luminance attenuation map for photometric uniformity in projection based displays. In *Proceedings of the ACM Symposium on Virtual Reality Software and Technology*, VRST '02, pp. 147–154. ACM, New York, NY, USA, 2002. doi: 10.1145/585740.585765

[17] A. Majumder and R. Stevens. Color nonuniformity in projection-based displays: analysis and solutions. *IEEE Transactions on Visualization and Computer Graphics*, 10(2):177–188, March 2004. doi: 10.1109/TVCG.2004.1260769

[18] A. Majumder and R. Stevens. Perceptual photometric seamlessness in projection-based tiled displays. *ACM Trans. Graph.*, 24(1):118–139, Jan. 2005. doi: 10.1145/1037957.1037964

[19] A. J. C. Moreira and M. Y. Santos. Concave hull: A k-nearest neighbours approach for the computation of the region occupied by a set of points. In *GRAPP (GM/R)*, pp. 61–68. INSTICC - Institute for Systems and Technologies of Information, Control and Communication, 2007.

[20] J. Morovic. Color gamut mapping. The Wiley series on imaging science and technology. Wiley, New York, 2008.

[21] J. Morovic and M. Luo. The fundamentals of gamut mapping: A survey. vol. 45, pp. 283–290, 2001. cited By 152.

[22] P. Prentašić, N. Mikša, A. Hedi, M. Subašić, and S. Lončarić. A method for projector brightness calibration for tiled displays. In *The 33rd International Convention MIPRO*, pp. 1379–1383, May 2010.

[23] R. Raskar, M. S. Brown, R. Yang, W.-C. Chen, G. Welch, H. Towles, B. Scales, and H. Fuchs. Multi-projector displays using camera-based registration. In *Visualization'99. Proceedings*, pp. 161–522. IEEE, 1999.

[24] R. Raskar, G. Welch, M. Cutts, A. Lake, L. Stesin, and H. Fuchs. The office of the future: A unified approach to image-based modeling and spatially immersive displays. In *Proceedings of the 25th Annual Conference on Computer Graphics and Interactive Techniques*, SIGGRAPH '98, pp. 179–188. ACM, New York, NY, USA, 1998. doi: 10.1145/280814.280861

[25] R. Raskar, G. Welch, K.-L. Low, and D. Bandyopadhyay. Shader lamps: Animating real objects with image-based illumination. In S. J. Gortler and K. Myszkowski, eds., *Rendering Techniques 2001*, pp. 89–102. Springer Vienna, Vienna, 2001.

[26] B. Sajadi, M. Lazarov, M. Gopi, and A. Majumder. Color seamlessness in multi-projector displays using constrained gamut morphing. *IEEE Transactions on Visualization and Computer Graphics*, 15(6):1317–1326, Nov 2009. doi: 10.1109/TVCG.2009.124

[27] B. Sajadi, M. Lazarov, and A. Majumder. Adict: Accurate direct and inverse color transformation. In K. Daniilidis, P. Maragos, and N. Paragios, eds., *Computer Vision – ECCV 2010*, pp. 72–86. Springer Berlin Heidelberg, Berlin, Heidelberg, 2010.

[28] G. Sharma, W. Wu, and E. N. Dalal. The ciede2000 color-difference formula: Implementation notes, supplementary test data, and mathematical observations. *Color Research and Application*, 30(1):21–30, 2005.

[29] C. Siegl, M. Colaianni, L. Thies, J. Thies, M. Zollhöfer, S. Izadi, M. Stamminger, and F. Bauer. Real-time pixel luminance optimization for dynamic multi-projection mapping. *ACM Trans. Graph.*, 34(6):237:1–237:11, Oct. 2015. doi: 10.1145/2816795.2818111

[30] A. Sireis and J. Kukal. Nonlinear smoothing of n-dimensional data using successive over-relaxation method. *Signal, Image and Video Processing*, 10(8):1497–1502, Nov 2016. doi: 10.1007/s11760-016-0961-y

[31] M. C. Stone. Color and brightness appearance issues in tiled displays. *IEEE Computer Graphics and Applications*, 21(5):58–66, Sep 2001. doi: 10.1109/38.946632

[32] J. Tsukamoto, D. Iwai, and K. Kashima. Radiometric compensation for cooperative distributed multi-projection system through 2-dof distributed control. *IEEE Transactions on Visualization and Computer Graphics*, 21(11):1221–1229, Nov 2015. doi: 10.1109/TVCG.2015.2459905

[33] G. Wallace, H. Chen, and K. Li. Color gamut matching for tiled display walls. In *Proceedings of the Workshop on Virtual Environments 2003*, EGVE '03, pp. 293–302. ACM, New York, NY, USA, 2003. doi: 10.1145/769953.769988

[34] G. Wetzstein and O. Bimber. Radiometric compensation through inverse light transport. In *Computer Graphics and Applications, 2007. PG '07. 15th Pacific Conference on*, pp. 391–399, Oct 2007. doi: 10.1109/PG.2007.47

[35] R. Yang, D. Gotz, J. Hensley, H. Towles, and M. S. Brown. Pixelflex: a reconfigurable multi-projector display system. In *Visualization, 2001. VIS '01. Proceedings*, pp. 167–554, Oct 2001. doi: 10.1109/VISUAL.2001.964508

[36] L. Zhang, S. Liang, B. Qin, and Z. Jiang. A three-phase approach to photometric calibration for multi-projector display using lcd projectors. In H. Zha, R.-i. Taniguchi, and S. Maybank, eds., *Computer Vision – ACCV 2009*, pp. 56–65. Springer Berlin Heidelberg, Berlin, Heidelberg, 2010.

[37] C. Zoido, J. Maroto, G. Romero, and J. Felez. Optimized methods for multi-projector display correction. *International Journal on Interactive Design and Manufacturing (IJIDeM)*, 7(1):13–25, Feb 2013. doi: 10.1007/s12008-012-0161-0